Application of Undersampling Technique for the Design of an NMR Signals Digital Receiver

GIULIO GIOVANNETTI,[1] VALENTINA HARTWIG,[1] VITTORIO VITI,[2] GIUSEPPE GAETA,[1] RAFFAELLO FRANCESCONI,[1] LUIGI LANDINI,[3] ANTONIO BENASSI[1]

[1] *Institute of Clinical Physiology, National Council of Research, Via Moruzzi 1, 56124 S. Cataldo, Pisa, Italy*
[2] *Esaote Biomedica s.p.a., Genova, Italy*
[3] *Department of Information Engineering, University of Pisa, Pisa, Italy*

ABSTRACT: In this article, undersampling technique theory and design, realization, and workbench test of a low-cost digital MRI (magnetic resonance imaging) receiver are reported. The authors first discuss classic analog receiver architecture, reporting its disadvantages, and then present a receiver with a complete description of the electronic circuit. The intended use of the subsystem should be as a radiofrequency (RF) receiver chain in a low-cost dedicated MRI scanner (e.g., suitable for musculoskeletal limbs studies). The digital receiver consists of a passband (antialiasing) filter, an ADC (analog to digital converter) to digitalize the signal with the undersampling technique, and a DDC (digital down converter) for the frequency translation and filtering to process the signal using a PC. The use of the DDC guarantees perfect signals quadrature and high-performance filtering; moreover, it is adaptable to each modification of the system because of its programmability. Detailed specifications and hardware design of the digital receiver that is designed to be used in a dedicated MR scanner is provided, guaranteeing top performance and low cost. Concepts Magn Reson Part B (Magn Reson Engineering) 29B: 107–114, 2006

KEY WORDS: undersampling; digital demodulator; radiofrequency signal; signal-to-noise ratio

INTRODUCTION

An MRI receiver is employed to convert the received RF signal from the coil into a suitable form for an ADC converter. Generally, the receiver is a superheterodyne circuit that demodulates the RF signal into a low-frequency band in accordance with a reference frequency equal to the emitted RF radiation (*1*).

Received 28 November 2005; revised 24 February 2006; accepted 27 February 2006

Correspondence to: Ing. G. Giovannetti, I.F.C., C.N.R.; E-mail: giovannetti@ifc.cnr.it

Concepts in Magnetic Resonance Part B (Magnetic Resonance Engineering), Vol. 29B(3) 107–114 (2006)

Published online in Wiley InterScience (www.interscience.wiley.com). DOI 10.1002/cmr.b.20065

The scheme of such classic analog MRI receiver is shown in Fig. 1. The free induction decay (FID) signal emitted by the sample is picked up by a RF coil and then processed by a circuit that maximizes the energy to transfer to the amplifier. The preamplifier amplifies the signal while minimizing the noise. The RF signal is then sent to a phase-quadrature detector system.

This type of receiver is simple, but it presents many problems. Filters and amplifiers must have the same phase and frequency characteristics, and there must be an extreme accuracy on 90° phase difference between the two reference signals. If not, a first-type distortion can occur ("ghost" artifacts on the image) (*2*). For these reasons, we implemented a phase-quadrature digital detector system that eliminates phase errors, unbalance errors, and ghost artifacts.

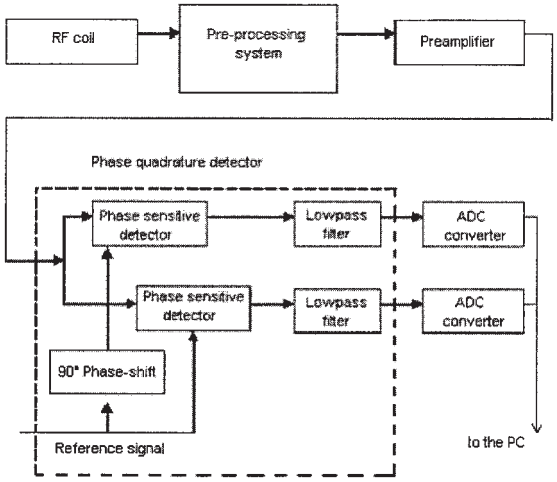

Figure 1 Block diagram of an MRI analog receiver.

Our low-cost digital receiver consists of a passband filter (antialiasing filter), an ADC to digitalize the signal with the undersampling technique, and a DDC (digital down converter) for the frequency translation and filtering to process the signal using a PC. We first explain the undersampling technique theory, then detail the hardware specifics of the circuit and provide test results of the device.

THEORY

Classical Analog MRI Receiver

The input of this detector is the MR radiofrequency signal represented by a frequency distribution around the transmission frequency f_0 (the Larmor's frequency); the detector translates it to a quantity equal to f_0 to center it around the zero frequency. This is the classic base-band detection, and it is obtained by multiplying the components of the MR signal with a reference signal at f_0 frequency. The phase-sensitive detector output is the sum of a component centered around zero frequency with another component centered around $2f_0$. A low-pass filter next removes the components centered around $2f_0$. Finally, the complex signal (two channels) is converted by two analog-to-digital converters for processing by PC (*3*).

Generally, the input signal of the NMR receiver has the following form:

$$S(t) = f(t)\cos(2\pi f_0 t) + jg(t)\sin(2\pi f_0 t), \qquad [1]$$

where f(t) and g(t) are the phase and quadrature components of the RF signal and f_0 is equal to the Larmor's frequency.

The RF signal is emitted by the nuclei in the object to be imaged and it is picked up by a RF receive coil. In our RF receiver chain we use a birdcage coil tuned at 7.66 MHz (corresponding to a static field of 0.18T) and an RF signal bandwidth of about 55 KHz (*4*).

Undersampling Technique

Generally, in a digital receiver, direct sampling (or passband sampling) is used: the signal is sampled without reporting it around the zero frequency (base band). In this case, the signal-to-noise ratio (SNR) is calculated by the following equation (*5*):

$$\mathrm{SNR} = 6.02\mathrm{N} + 1.76\ \mathrm{dB} \qquad [2]$$

where N is the ADC converter bit number.

To increase SNR, an oversampling technique can be used. Oversampling methods for analog-to-digital converters are based on sampling an analog signal at a much higher rate, filtering the samples with a digital low-pass filter, and reducing the sample rate by decimation. In this case, the equation for SNR is

$$\mathrm{SNR} = 6.02\mathrm{N} + 1.76\ \mathrm{dB} + 10\log\left(\frac{f_s}{2B}\right) \qquad [3]$$

where f_s is the sampling frequency, which must be greater than double the signal maximum frequency (according to Nyquist's theory), and B is the signal bandwidth.

As the sampling frequency increases, the noise tends to decrease because it is distributed on a greater range of frequency (Fig. 2), so the SNR increases. The term for this phenomenon is "process gain" and it provides a 3-dB increment for each doubling of f_s frequency.

As described previously, the output signal of the RF coil has a central frequency of 7.66 MHz and a

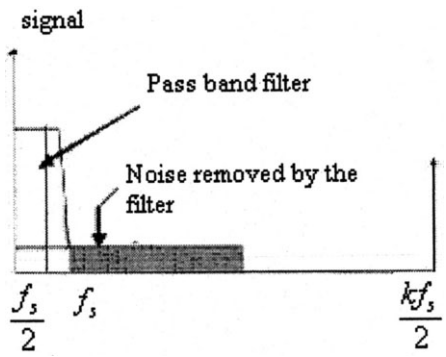

Figure 2 Oversampling effect on the noise.

bandwidth of about 55 KHz. Therefore, with oversampling, the signal has to be sampled at a frequency greater than 2×7.66 MHz. Otherwise, an innovative technique defined as "undersampling" or "super-Nyquist" configuration can be used, where the sampling rate is determined only by the signal bandwidth.

Shannon's theorem establishes that a signal with a maximum frequency of f_a must be sampled by a sampling frequency $f_s > 2f_a$ to avoid loss of information. A consequent of this theorem is Nyquist's criteria: if $f_s < 2f_a$, you have aliasing, which is the noise caused by the overlapped signal replicas.

This criteria is valid when the signal extends from zero frequency to f_a, but if the signal does not extend from DC (direct current), the sampling rate depends on both its band and its position on the frequency spectrum. Therefore, Nyquist's criteria establishes that f_s must be greater than $2B$, where $B = f_2 - f_1$ is the signal bandwidth. Because Nyquist's band is defined as the frequency range from zero to $f_s/2$, the frequency spectrum can be subdivided into many Nyquist's zones with amplitude of $0.5\ f_s$. In general, the sampling of a signal with B band at a rate of f_s causes two components of aliasing: one at f_s + B and another at f_s − B.

By the effect of the sampling, a signal replica (or the signal itself) falls into the first Nyquist's zone ($0 - f_s/2$). For this reason, every signal (noise or useful signal) that falls out of the interesting band must be filtered before the sampling. Therefore, an important part of the receiver is the bandpass filter.

In the undersampling technique, the aliasing phenomenon is an advantage: the signal replica that falls in the first Nyquist's zone contains all original signal information (*7*). Obviously, the band of the original signal must be limited to a single Nyquist's zone by the bandpass filter (anti-aliasing filter).

The sampling frequency f_s must be chosen considering the following two expressions: 1) $f_s > 2B$, which is the super Nyquist condition (where B is the signal band), and 2) $f_s = \dfrac{4f_c}{2NZ - 1}$, where f_c is the signal central frequency and NZ is the Nyquist's zone (NZ = 1, 2, 3. . .). The second equation ensures that f_c is in the center of a Nyquist's zone.

As described in the next section, for our application we used a 3 MSPS ADC. With a sampling frequency of 2.7648 MSPS, which we obtained by dividing a commercial oscillator frequency (11.0592 MHz) by four, the signal falls into the sixth Nyquist's zone. To calculate where the aliased signal falls, the following equation can be used:

$$f_c \mod f_s \qquad [4]$$

and in our case

$$7.66 \text{ MHz} \bmod 2.7648 \text{ MHz} = 2.1304 \text{ MHz}. \qquad [5]$$

This frequency value lies in the second Nyquist's zone; therefore, the signal must be translated in the center of the first Nyquist's zone, using a DDC, which acts like a phase quadrature detector.

The DDC control software calculates the translation frequency using the following expression:

$$3f_s - f_c = 634.4 \text{ KHz}. \qquad [6]$$

The sampling frequency that we chose allows us to space out the replicas in the frequency spectrum to relax the anti-aliasing filter performance and to reach an oversampling factor equal to

$$10 \log\left(\frac{f_s}{2B}\right) = 14 \text{ dB}. \qquad [7]$$

This is the minimum value for the oversampling factor; in fact, the received signal bandwidth B is also related to the FOV and the frequency encoding gradient, G_f, according to the equation (*8*)

$$\text{FOV} = \frac{B}{\gamma G_f}. \qquad [8]$$

In our case, with a gradient magnetic field of 0.5 G/cm and γ = 42.58 MHz/T for the hydrogen atom, the FOV is equal to

$$\frac{55 \text{ KHz}}{42.58 \text{ MHz/T} \times 0.5 \cdot 10^{-4} \text{ T/cm}} = 25 \text{ cm} \qquad [9]$$

with a process gain values of 14 dB (see Eq. [7]).

If the FOV is smaller and the product γG_f remains constant, the signal bandwidth decreases while the process gain increases. For our intended use of dedicated MRI for musculoskeletal limbs studies, a standard FOV value is equal to 10 cm and the bandwidth calculation provides

$$B = \text{FOV} \times \gamma G_f = 21.29 \text{ KHz}. \qquad [10]$$

In accordance with Eq. [7], the process gain is

$$10 \log \frac{2.7648 \text{ MHz}}{2 \times 21.29 \text{ KHz}} \cong 18 \text{ dB}. \qquad [11]$$

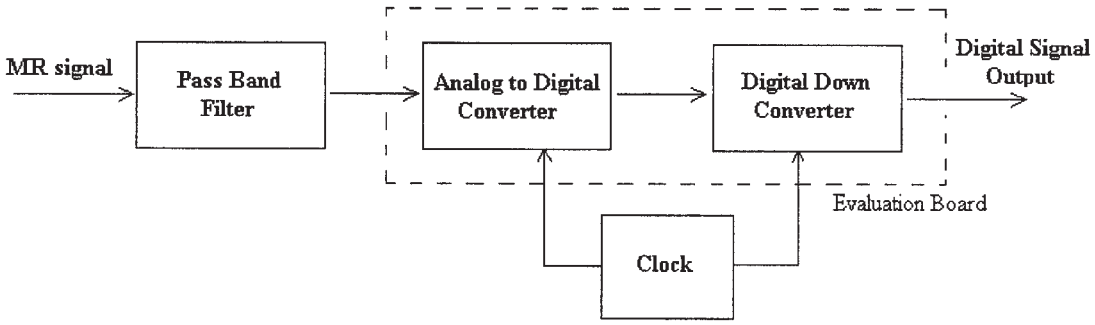

Figure 3 Block diagram of an MRI digital receiver.

ADC Specifications

The undersampling technique requires that the ADC has low distortion at the frequency of interest. In such an application, the design of the ADC has to consider spurious-free dynamic range (SFDR), defined as the difference in decibels between the root mean square (RMS) value of the input signal amplitude and the peak of the noise signal, and the ENOB (effective number of bit), defined by the following equation (*7*):

$$\mathrm{ENOB} = \frac{\mathrm{SINAD} - 1.76}{6.02} \qquad [12]$$

where signal to noise and distortion (SINAD) is defined as

$$\mathrm{SINAD} = -20\log\left(\sqrt{(10^{-\mathrm{SNR}/10} + 10^{\mathrm{THD}/10})}\right) \qquad [13]$$

and THD is the total harmonic distortion.

Therefore, the SINAD is defined as the ratio between the RMS value of the input signal and the RMS value of the other spectral components under Nyquist's frequency sum, including all harmonics without the DC components. The SNR is defined as the ratio between the RMS value of the input signal and the RMS value of the first six harmonics sum, including the DC components.

MATERIALS AND METHODS

Hardware

In an MR spectrometer, the FID signal is detected by a receiver coil (birdcage, in our application) and by a preprocessing system. The signal is sent to a preamplifier, which maximizes the SNR. Successively, a variable gain amplifier adapts the signal to the input dynamic of the ADC converter. Figure 3 shows the block diagram of the designed digital MR receiver. The first block is a passband filter, which eliminates the undesired frequency outside the interesting band. The ADC converter digitalizes the signal for the last block—the digital demodulator DDC that performs the frequency translation, frequency decimation, and digital filter.

The chosen sampling frequency (f_s = 2.7658 MHz) allows the signal to be centered in a Nyquist's zone. After the sampling, the aliased signal falls in the second Nyquist's zone (using Eq. [4]). Therefore, to obtain the exact position of the signal in the first Nyquist's zone, the DDC must perform a frequency translation of 634.4 KHz according to Eq. [6] (Fig. 4).

Passband Filter. After a comparison of the transition band shape and stopband attenuation for various filter typology, we designed a sixth-order elliptic passive passband filter to achieve a good attenuation in the Nyquist's zone corresponding to the interesting signal. Figure 5 shows the passband filter scheme. The input/output resistors are characteristic of the coaxial cable used to transmit and capture the signal. Table 1 shows the electric components values of the built filter. The specifics obtained by the built filter are passband = 300 kHz; passband attenuation = 2 dB;

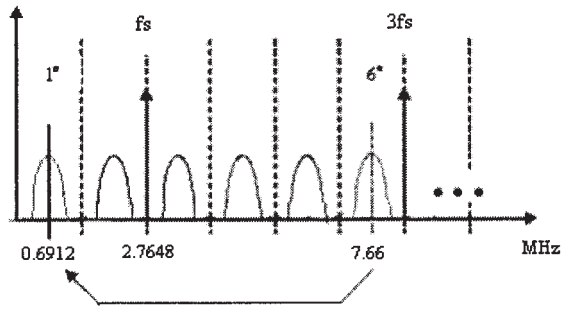

Figure 4 The aliased signals after undersampling application.

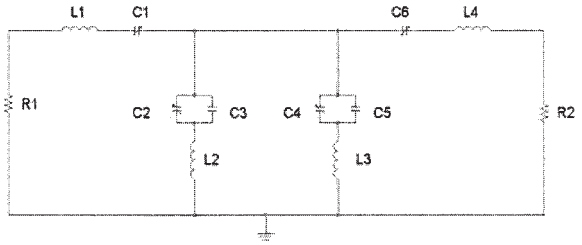

Figure 5 Electric scheme of the passband filter.

stopband = 1.25 MHz; and stopband attenuation = 40 dB.

Analog-to-Digital Converter. In this work, we used a low-cost AD9243 analog-to-digital converter characterized by a maximum sampling rate of 3 MSPS and a dynamic of 14 bit (*9*). This converter uses a four-block pipeline architecture with an input sample-and-hold amplifier (SHA) with wide band. It has a SINAD of 77 dB and an SNR of 80 dB at our frequency of interest (f_c = 7.66 MHz).

Digital Down Converter. The digital down converter (DDC) provides the following functions on the ADC output samples: frequency translation, frequency decimation, and digital filter. For our application, we chose a low-cost component with programmable bandwidth and decimation, the AD6620, which is characterized by four main signal processing stages: 1) a frequency translator; 2) and 3) two cascaded integrator combo FIR filters (CIC2, CIC5; fixed coefficients decimator filters); and 4) a RAM coefficient FIR filter (RCF; a programmable coefficient decimator filter) (*10*).

The first signal processing stage is a frequency translator consisting of two multipliers and a 32-bit complex numerically controlled oscillator (NCO). The NCO serves as a quadrature local oscillator capable of producing any frequency between $-f_s/2$ and $+f_s/2$ with a resolution of $f_s/2^{32}$.

The control word, NCO_FREQ, is interpreted as a 32-bit unsigned integer. To translate a signal centered at f_c to zero frequency, NCO_FREQ can be calculated using the following equation:

$$\text{NCO\_FREQ} = 2^{32} \times \text{mod}\frac{f_C}{f_S} \qquad [14]$$

The second stage consists of a fixed coefficient decimator filter; it is represented by a second-order CIC filter (CIC2) consisting of two cascaded integrators followed by a decimation and two derivators.

The third stage is a fifth-order CIC filter (CIC5), necessary to reduce the input data rate at

$$f_{S5} \leq \frac{f_{S2}}{M_{\text{CIC5}}} \qquad [15]$$

where M_{CIC5} is programmable between a value of 1 and 32 and f_{S2} is the output data rate of the filter CIC2:

$$f_{S2} = \frac{f_S}{M_{\text{CIC2}}} \qquad [16]$$

where M_{CIC2} is programmable between a value of 0 and 6.

The final signal processing stage is a sum-of-products decimating filter with programmable coefficients, and the final response of the AD6620 is the combination of three cascaded filters responses, where each stage allows more and tighter transition bands.

Clock System. The clock signal is employed to interrogate the device input port and to synchronize the successive processing stages. In our system, we used a hybrid commercial oscillator SCO-020 with a frequency of 11.0592 MHz and a phase-locked loop (PLL) MC88915 with a frequency ratio of 1:2, 1:1, and 2:1 with respect to the input frequency (*11*).

The external loop filter is a homemade large-band filter that decreases the device sensibility to power oscillation typical of a high-frequency digital system (*12*).

Evaluation Boards. Principal components of our digital receiver (AD6620 and AD9243) are available as evaluation boards. The input data of the AD6620 evaluation board are processed by two latches (74LCX574) successively. They are available in real

Table 1 Electric Components Values of the Built Passband Filter

Component	Value
R_1	50 Ω
L_1	27 μH
C_1	16 pF capacitive trimmer Voltronics JB series
C_2	49 pF capacitive trimmer Voltronics JB series
C_3	820 pF multilayer capacitor ATC 100E series
L_2	706 nH
C_4	53 pF capacitive trimmer Voltronics JB series
C_5	560 pF multilayer capacitor ATC 100E series
L_3	498 nH
C_6	16 pF capacitive trimmer Voltronics JB series
L_4	27 μH
R_2	50 Ω

time to be processed by a microprocessor (serial or parallel output) or stored in a first input/first output (FIFO) memory and then downloaded on PC by the parallel port (*13*).

The evaluation board provides a bypass modality; in this way, the AD6620 is excluded. The data input flow through a second series of latches and are successively memorized by the FIFO memory to be processed later. This allows verification of the AD9243 function. Moreover, in the evaluation board, some jumpers allow a delay so that the correct temporization of the device can be obtained.

Software

AD6620 Simulation Software. The AD6620 simulation software allows for the digital filters specifics (passband, stopband, and attenuations). The signal bandwidth is B = 21.29 kHz; therefore, the final decimation filter factor must be equal to

$$\frac{f_S}{2 * \mathrm{B}} = \frac{2.7648\ \mathrm{MHz}}{2 * 21.29\ \mathrm{kHz}} = 64.9. \qquad [17]$$

Because the decimation factor must be an integer, we chose a bandwidth equal to 21.6 KHz.

Moreover, we established that the final digital filter must have the following specifics: passband = 21.6 kHz and passband attenuation = 0 dB. After the setting up of sampling parameters, the software calculates the decimation factors of the three filters CIC2, CIC5, and RCF to obtain the requested specifics.

AD6620 Evaluation Board Software. To control the AD6620 we used the evaluation board support software. The software graphic interface consists of two windows: the AD6620 monitor and the AD6620 controller, which allows the user to set up the AD6620 parameters and download the data from the FIFO memory to the PC.

The AD6620 controller allows the user to set up all functional parameters as the data input modality (in our case, single channel real), the sampling rate, the shift frequency value of NCO (automatically set up), and the configuration of the digital filters (CIC2, CIC5, RCF). The AD6620 monitor allows the user to control and process the FIFO memory data—in particular, analysis of the data FFT (fast Fourier transform), their value in the time domain, and the I versus Q graphic (phase and quadrature components of data). It also allows evaluation of the SINAD and SNR values, the second and third harmonic level of the wider signal in the spectrum (in dBc), and the level of the successive spurious wider signal measured with respect to the full scale (in dBFS).

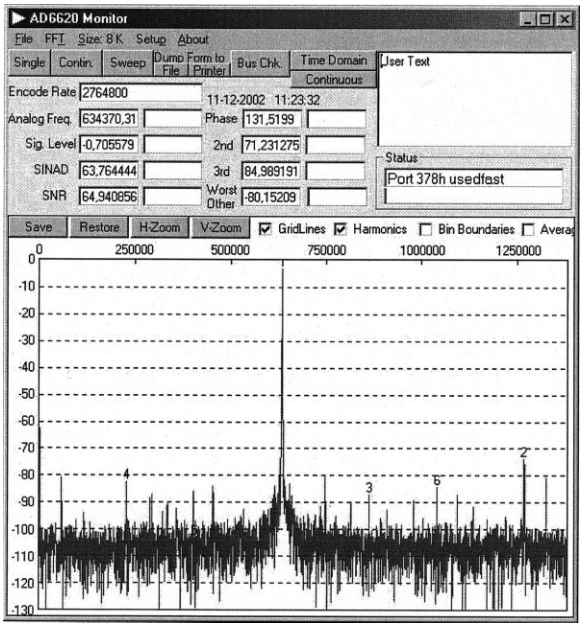

Figure 6 ADC output signal FFT for an input sinusoid with a frequency of 7.66 MHz.

RESULTS

For the receiver testing, we used a function generator (HP3325A, Hewlett Packard) providing, as input signal, a sinusoidal wave at Larmor's frequency (f_0 = 7.66 MHz) with an amplitude near to the full-scale value of the converter ($\cong -0.5$ dBFS on 2 Vpp) to maximize its performance.

In the first measurement, we bypassed the DDC for the evaluation of the ADC output signal FFT. The digitalized signal spectrum, obtained by the evaluation board software, is shown in Fig. 6. The performance of the analog-digital converter is as follows: SINAD = 63.76 dB; SNR = 64.94 dB; second harmonic level with respect to the principal component = −71.23 dBc; third harmonic level with respect to the principal component = −84.99 dBc. Successively, we evaluated the complete system, composed of the ADC and the DDC, choosing a digital signal bandwidth (B) equal to 21.6 kHz.

Figure 7 represents the module of the FFT of the complex output signal obtained by the NCO of the AD6620. The AD6620 centered the fundamental component of the signal around the zero frequency,

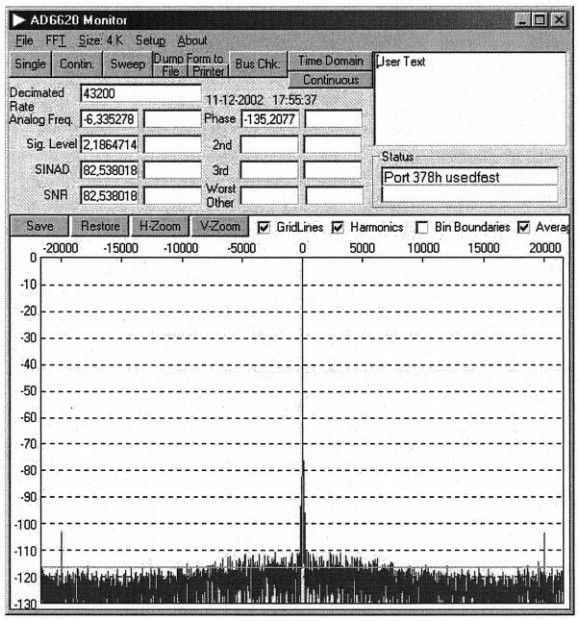

Figure 7 DDC output complex signal FFT module.

guaranteeing a processing gain that provides a signal-to-noise ratio equal to

$$\text{SINAD} = \text{SNR} = 82.54 \text{ dB}. \qquad [18]$$

Another important benefit of the digital demodulator is that it allows the user to obtain a perfect quadrature of the two signals and to reduce ghost artifacts.

DISCUSSION

In this article, we used the undersampling technique for the design of a low-cost NMR signals receiver system for the demodulation of a passband signal centered at the frequency of 7.66 MHz and with a band of 55 kHz. The intended use of our subsystem is as an RF receiver chain in a low-cost dedicated MRI scanner (e.g., in a machine for musculoskeletal limbs studies).

The signal digitalizing process acts as a method to elaborate the signal with excellent performance with respect to an analog receiver system. The ADC test shows dynamic performance characterized by a SINAD of about 63.8 dB and an SNR of about 65 dB. Using the DDC as a phase quadrature detector and digital filter, an SNR value of about 83 dB was obtained. This provides increased performance, guaranteeing the perfect quadrature of the phase and quadrature parts of the input signal, and high-performance filtering, which results in a reduction in ghost artifacts that often affect the MR images obtained with a classic receiver. Moreover, it is easily adaptable to each modification of the system thanks to its programmability.

The described system is designed to be used with a single-channel RF input received by a birdcage coil: in this case, the DDC output is composed of the phase and quadrature components of the digitalized signal that are used by the PC to reconstruct the MR image. However, the system can be used with a two-channel receiver coil to enhance the SNR of the final results.

The designed receiver can easily be integrated into a low-cost imager, generally based on a PC platform, because the control of the AD6620 evaluation board occurs through the PC parallel port (*13*).

The usefulness of undersampling in the acquisition of magnetic resonance signals has already been demonstrated in the literature (*6*). We reported here the theory of this technique and described in detail all components of such a digital receiver so that the low-cost architecture can be completely homemade. The undersampling technique could provide an SNR similar to that obtained with an analog phase-quadrature detector, but with minimal phase errors, unbalance errors, and ghost artefacts (*14*).

The advent of recent ADCs makes possible the use of direct signal sampling at low magnetic fields, such as low frequency. However, using the undersampling technique, the different elements of the receiver chain (i.e., passband filter) have more relaxed specifics (e.g., compared with a direct sampling method) with several design advantages (e.g., low cost of entire architecture).

REFERENCES

1. Jin J. 1999. Electromagnetic analysis and design in magnetic resonance imaging. Boca Raton, FL: CRC Press.
2. Kasal M, Halamek J, Husek V, Villa M, Ruffina U, Cofrancesco P. 1994. Signal processing in transceivers for nuclear magnetic resonance and imaging. Rev Sci Instrum 65:1897–1902.
3. Chen C, Hoult DJ. 1989. Biomedical magnetic resonance technology. Bristol: IOP.
4. Giovannetti G, Francesconi R, Landini L, Santarelli MF, Positano V, Viti V, et al. 2004. Conductors geometry and capacitors quality for performance optimization of low frequency birdcage coils. Concepts Magn Reson Part B Magn Reson Eng 20B:9–16.
5. Villa M, Tian F, Cofrancesco P, Halàmek J, Kasal M. 1996. High resolution digital quadrature detection. Rev Sci Instrum 67:2123–2129.
6. Perez P, Santos A, Vaquero JJ, Rivera M, Del Pozo F. 1996. Reducing analog circuitry by sampling NMR signals at low speeds. MAGMA IV(II):100.

7. Kester W. Undersampling applications. Available at: http://www.analog.com/Analog_Root/static/pdf/amplifiersLinear/training/Section5.pdf
8. Hornak JP. The basics of MRI. Available at: http://www.cis.rit.edu/htbooks/mri
9. AD9243 Data sheet, analog device. Available at: http://www.analog.com/UploadedFiles/Data_Sheets/743220193AD9243_a.pdf
10. AD6620 Data sheet, analog device. Available at: http://www.analog.com/UploadedFiles/Data_Sheets/180387430AD6620_a.pdf
11. SCO-020 Data sheet, Sunny Electronics. Available at: http://www.sunny.co.kr/en/products/pro02.htm
12. MC88915 Data sheet, Motorola. Available at: http://www.physi.uni-heidelberg.de/physi/ceres/electronics/datasheets/mc88915rev3–1.pdf
13. AD6620 Evaluation board manual, analog device. Available at: http://people.ece.cornell.edu/wes/Projects/Ad6620ev.pdf
14. Perez P, Santos A. 2004. Undersampling to acquire nuclear magnetic resonance images. Med Engin Phys 26:523–529.